

## RESEARCH ARTICLE

# A lethal fungal pathogen directly alters tight junction proteins in the skin of a susceptible amphibian

Julia Gauberg<sup>1,2,\*</sup>, Nicholas Wu<sup>1</sup>, Rebecca L. Cramp<sup>1</sup>, Scott P. Kelly<sup>2</sup> and Craig E. Franklin<sup>1,‡</sup>

## ABSTRACT

Bacterial and viral pathogens can weaken epithelial barriers by targeting and disrupting tight junction (TJ) proteins. However, comparatively little is known about the direct effects of fungal pathogens on TJ proteins and their expression. The disease chytridiomycosis, caused by the fungal pathogen *Batrachochytrium dendrobatidis* (*Bd*), is threatening amphibian populations worldwide. *Bd* is known to infect amphibian skin and disrupt cutaneous osmoregulation. However, exactly how this occurs is poorly understood. This study considered the impact of *Bd* infection on the barrier properties of the Australian green tree frog (*Litoria caerulea*) epidermis by examining how inoculation of animals with *Bd* influenced the paracellular movement of FITC-dextran (4 kDa, FD-4) across the skin in association with alterations in the mRNA and protein abundance of select TJ proteins of the epidermal TJ complex. It was observed that *Bd* infection increased paracellular movement of FD-4 across the skin linearly with fungal infection load. In addition, *Bd* infection increased transcript abundance of the tricellular TJ (tTJ) protein tricellulin (Tric) as well as the bicellular TJ (bTJ) proteins occludin (Ocln), claudins (Cldn)-1, Cldn-4 and the scaffolding TJ protein zonula occludens 1 (ZO-1). However, while Tric protein abundance increased in accord with changes in transcript abundance, protein abundance of Cldn-1 was significantly reduced and Ocln protein abundance was unchanged. Data indicate that disruption of cutaneous osmoregulation in *L. caerulea* following *Bd* infection occurs, at least in part, by an increase in epidermal paracellular permeability in association with compromised integrity of the epidermal TJ complex.

**KEY WORDS:** Chytrid fungus, *Batrachochytrium dendrobatidis*, Paracellular permeability, Claudin, Occludin, Tricellulin

## INTRODUCTION

Solute movement across epithelial barriers is dictated by (1) the transcellular transport pathway, which moves ions against their concentration gradient across epithelial cells, and (2) the paracellular transport pathway, which regulates the passive movement of solutes down a concentration gradient across tight junctions (TJs) that occlude the juxtaluminal paracellular space between epithelial cells (Martinez-Palomo et al., 1971; Ehrenfeld and Klein, 1997). The TJ complex is composed of cytosolic


scaffolding [e.g. zonula occludens 1 (ZO-1)] and transmembrane [e.g. claudins (Cldns), occludin (Ocln), tricellulin (Tric)] TJ proteins (Günzel and Fromm, 2012; Fig. 1). Cytosolic scaffolding TJ proteins like ZO-1 link transmembrane TJ proteins to the cellular cytoskeleton and participate in the dynamic assembly of the TJ complex (Gonzalez-Mariscal et al., 2003). In contrast to scaffolding TJ proteins, transmembrane TJ proteins possess extracellular domains. Transmembrane TJ proteins that link two adjacent cellular membranes are termed bicellular TJ (bTJ) proteins, while those found at tricellular points of contact are referred to as tricellular TJ (tTJ) proteins (Raleigh et al., 2010). Cldns are a large superfamily of bTJ proteins that can influence the paracellular permeability of an epithelium by forming ion-selective barriers or pores (Günzel and Fromm, 2012). The expression of Cldns in cells is sufficient to form TJ strands, and loss of just one Cldn protein may greatly affect the paracellular permeability of an epithelium (Furuse et al., 1998, 2002). Other important transmembrane TJ proteins include TJ-associated MARVEL proteins such as the bTJ protein Ocln (Furuse et al., 1993) and the tTJ protein Tric (Ikenouchi et al., 2005). Ocln arose in deuterostomes as an important structural protein for normal barrier function (Chapman et al., 2010) and it has been found in the epithelia and/or endothelia of many terrestrial and aquatic vertebrate groups (Feldman et al., 2005; Chasiotis and Kelly, 2008, 2009; Kolosov et al., 2017a). Tric seals the hollow ‘tube’ that is formed perpendicular to the epithelium surface in regions where three epithelial cells meet (Ikenouchi et al., 2005). Tric has been reported to restrict the passage of solutes and contribute to epithelium integrity in mammals and fishes (Ikenouchi et al., 2005; 2009; Kolosov and Kelly, 2013, 2018).

Epithelial barriers are generally effective at inhibiting pathogen entry into tissues; however, various bacterial and viral pathogens are well known to disrupt and target TJ proteins in order to weaken the epithelial barrier (for a review, see Guttman and Finlay, 2009). Some bacterial and viral pathogens destroy TJ proteins (Muza-Moons et al., 2004; Köhler et al., 2007), whereas others, such as *Clostridium perfringens* and hepatitis C virus, target specific TJ proteins as receptors for tissue entry (Katahira et al., 1997; Evans et al., 2007; Robertson et al., 2010; Sourisseau et al., 2013). The effects of fungal pathogens (in contrast to bacterial and viral pathogens) on TJ proteins have only been examined in a handful of studies (McLaughlin et al., 2004, 2009; Yuki et al., 2007). As a result, we have limited knowledge on the interaction of fungi and fungal toxins with the TJ complex. Understanding the fungus–TJ interaction is especially important in light of an emerging infectious disease, chytridiomycosis, that disrupts the skin function of amphibians.

Chytridiomycosis is a cutaneous infection in amphibians caused by the pathogenic fungus *Batrachochytrium dendrobatidis* (*Bd*) (Stuart et al., 2004). This fungus has been shown to infect over 500 amphibian species worldwide and has resulted in one of the greatest disease-driven losses of biodiversity ever recorded (Fisher et al., 2009; Kilpatrick et al., 2010). Although only the superficial layers

<sup>1</sup>School of Biological Sciences, The University of Queensland, Brisbane, QLD 4072, Australia. <sup>2</sup>Department of Biology, York University, Toronto, ON, Canada M3J 1P3. <sup>\*</sup>Present address: Department of Cell and Systems Biology, University of Toronto Mississauga, Mississauga, ON, Canada L5L 1C6.

<sup>‡</sup>Author for correspondence (c.franklin@uq.edu.au)

 J.G., 0000-0002-9249-9659; N.W., 0000-0002-7130-1279; C.E.F., 0000-0003-1315-3797

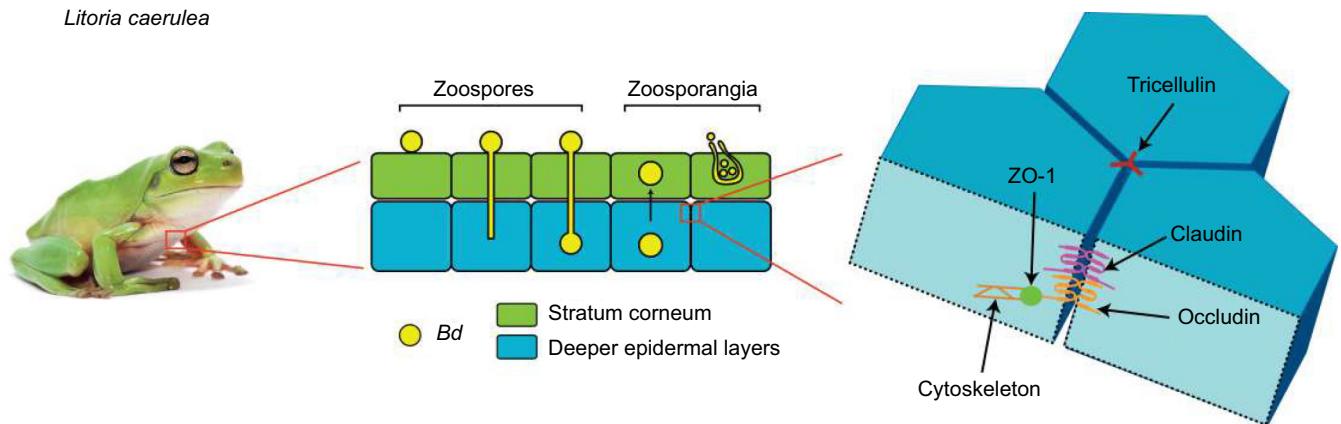


**Fig. 1. Schematic representation of the *Batrachochytrium dendrobatidis* (*Bd*) life cycle in the amphibian epidermis and location of the tight junction (TJ) complex in the epidermis.** The stages of *Bd* infection have been summarized by Van Rooij et al. (2015) and are as follows: (1) the fungus encysts on to the outer layer of the skin (the stratum corneum), (2) the zoospore sends a germ tube into the deeper layers of the skin, (3) *Bd* injects itself into a living epidermal cell, (4) the zoospore develops into a zoosporangia as the skin cells are pushed upwards and mature, and (5) zoosporangia develop a discharge tube from which new zoospores are released. A schematic diagram of the location of the cytosolic (ZO-1), bicellular (Occludin, Claudin) and tricellular (Tricellulin) TJ proteins in the vertebrate epidermis is also shown. Photo credit: C. Baker.

of the skin are infected by *Bd*, that alone is enough to disrupt normal skin function and can lead to death of the infected animal (Voyles et al., 2009). This is because in amphibians, the skin, specifically the ventral skin surface, is a selectively permeable living barrier to the surrounding environment that plays an important (sometimes exclusive) role in gas exchange and is a predominant site for salt and water transport (Parsons and Mobin, 1991; Boutilier et al., 1992; Hillyard et al., 2008; Campbell et al., 2012).

The mechanism used by *Bd* to infect amphibian skin is still not completely understood (Rosenblum et al., 2008; Fisher et al., 2009). What is known is that the fungus begins its life cycle as a free-living zoospore which encysts onto the surface of the skin (Van Rooij et al., 2015; Fig. 1). The zoospore then develops a germ tube that forces its cell contents into the deeper layers of the skin (Van Rooij et al., 2015). Finally, *Bd* matures into zoosporangia containing many zoospores that can be shed from the skin via a discharge tube to re-infect the same animal, or infect a new one (Greenspan et al., 2012; Van Rooij et al., 2015). Following infection, *Bd* has been reported to affect active solute transport and transepithelial resistance (TER) across the ventral skin, disrupting cutaneous osmoregulation and causing an imbalance in serum ion levels (Voyles et al., 2007, 2009; Wu et al., 2018). TER is a measure of transcellular and paracellular transport and, while both pathways contribute to the barrier properties of the amphibian epidermis, the paracellular route heavily influences its permeability properties (e.g. Cox and Alvarado, 1979). Although the effects of *Bd* have been examined on active ion transport and TER, the effects of *Bd* on paracellular transport and TJs specifically have not been investigated.

TJs are acknowledged to play a vital role in determining paracellular resistance of terrestrial and aquatic vertebrate epithelia (Chasiotis et al., 2012a; Günzel and Fromm, 2012; Kolosov et al., 2017b; Kolosov and Kelly, 2017, 2018), including amphibian skin (Mandel and Curran, 1972; Bruus et al., 1976). Additionally, amphibian TJs, and at least three proteins of the amphibian TJ complex (i.e. Cldn-1, Ocln, ZO-1), have been shown to respond to changes in environmental conditions (Castillo et al., 1991; Chasiotis and Kelly, 2009; Tokuda et al., 2010). Over 30 genes encoding amphibian TJ proteins have now been reported, yet little is known about their contribution to TJ permeability (Cardellini et al., 1996; Cordenonsi et al., 1997; Fesenko et al., 2000; Klein et al., 2002;

Chasiotis and Kelly, 2009; Chang et al., 2010; Saharinen et al., 2010; Yamagishi et al., 2010; Baltzegar et al., 2013; Sun et al., 2015). In addition, the majority of these genes have been identified in the strictly aquatic anurans *Xenopus laevis* and *Xenopus tropicalis*; thus, almost nothing is known about the characteristics of TJ proteins in terrestrial and semi-aquatic amphibians (Günzel and Yu, 2013). There is considerable evidence that a dysregulation of TJ function can deleteriously impact normal solute movement across epithelia that interface directly with the surrounding environment of aquatic vertebrates (Chasiotis et al., 2012b; Kolosov and Kelly, 2013, 2017, 2018; Kolosov et al., 2017b), so it would seem prudent to carefully consider the effect of *Bd* on epidermal TJs of amphibians. Indeed, it has been demonstrated that *Bd* disrupts junctional components responsible for adhesion between cells of amphibian skin, resulting in skin lesions (Brutyn et al., 2012). But, unlike TJs, adhesion junctions do not regulate the permeability properties of the skin. Furthermore, several fungi and fungal toxins have been shown to directly target and disrupt various junctional components, including TJs, in the skin of other vertebrates (Bouhet and Oswald, 2005; Yuki et al., 2007). Additionally, *Bd* was found to secrete proteolytic enzymes, which are hypothesized to be linked to its pathogenicity (Rosenblum et al., 2008; Symonds et al., 2008) and may contribute to skin barrier disruption as reported by Brutyn et al. (2012) for the skin of *X. laevis*.

Given that fungal toxins have been shown to target vertebrate TJs and that *Bd* has been found to affect cutaneous osmoregulation as well as disrupt junctional adhesion components in the skin of amphibians, it was hypothesized that the disruption of amphibian cutaneous osmoregulation following *Bd* infection will occur in association with altered epidermal paracellular permeability and TJ protein abundance. To consider this idea further, ventral skin permeability and TJ protein abundance of the Australian green tree frog, *Litoria caerulea*, were examined following experimental infection with *Bd*.

## MATERIALS AND METHODS

### Experimental animals

This study was conducted using the Australian green tree frog *Litoria caerulea* (White 1790), which is susceptible to *Bd* infection and is a model for the study of chytridiomycosis (Pessier et al., 1999; Berger et al., 2005; Voyles et al., 2009; Wu et al., 2018). All animals

were collected with approval of the Queensland Department of Environment and Heritage Protection (WISP15102214), and all experiments were carried out with the approval of The University of Queensland Animal Welfare Committee (SBS/316/14/URG). Specifically, *L. caerulea* (15–70 g, mixed sex) were collected from wet roads in non-protected areas near Fernvale, southeast Queensland, in January 2015. Isolated individual frogs were placed into separate moistened plastic bags and transported to The University of Queensland. Frogs were housed separately in ventilated clear plastic containers (26.2×23.7×12 cm). Containers were supplied with paper towels saturated with water that was chemically aged (dilution 1:4000; VitaPet, Sydney, NSW, Australia) and each housing unit contained a half PVC pipe for shelter. Frogs were fed large crickets (5 each week) and the enclosures were cleaned on a weekly basis. Photoperiod was maintained on a 12 h light:12 h dark cycle and room temperature was kept constant at 20.5±0.5°C. Given that natural *L. caerulea* populations can acquire *Bd* infections, swabs taken from captured frogs were tested for *Bd* using Taqman real-time PCR (qPCR) prior to beginning the experiments and all frogs were confirmed to be uninfected.

### Preparation of fungal inoculum and experimental exposure

*Bd* strain EPS4, isolated by E. P. Symonds (School of Veterinary Sciences, The University of Queensland) from a *Mixophyes fleayi* tadpole collected from Gap Creek, Main Range National Park, QLD, Australia (March 2012), was used for experimental infection. *Bd* cultures were maintained at 4°C until 4 days before exposure date. The strain was then passaged onto 25 new 1% agar, 0.5% tryptone, 0.5% tryptone-soy plates, and maintained at 20°C for 4–5 days. Immediately prior to infection, zoospores maintained at 20°C were harvested by flooding plates with sterile distilled water for 30 min. The zoospore suspension was collected, and zoospore concentration was calculated using a haemocytometer following Boyle et al. (2004). Frogs were randomly assigned to be part of either the infected ( $n=10$ ) or the control ( $n=10$ ) group. All frogs were transferred into 300 ml plastic containers (12.5×8.3×5 cm) containing 100 ml of aged tap water. Frogs in the infected group were then inoculated with a dose of ~500,000 *Bd* zoospores, which was added to their skin and surrounding water, for 5 h. Control frogs were exposed to identical conditions in the absence of zoospores. After exposure, frogs were returned to their original enclosures. All experiments were conducted when frogs were in the non-sloughing cycle.

### Measuring infection load

The swabbing protocol used to determine the presence or absence of *Bd* on collected animals as well as *Bd* infection load on inoculated animals (every 2 weeks after exposure) involved firmly running a sterile fine-tipped cotton swab (MW100-100; Medical Wire and Equipment, Corsham, Wiltshire, UK) three times over the frog's ventral surface, sides, thighs, feet, webbing and toes. Fungal DNA was isolated using PrepMan Ultra (Applied Biosystems, Foster City, CA, USA) according to manufacturer's instructions (Qiagen Pty Ltd, Chadstone, VIC, Australia) and assayed in triplicate via Taqman qPCR (Boyle et al., 2004) using a Mini Opticon qPCR detection system (MJ Mini Cycler, Bio-Rad Laboratories, Inc., Hercules, CA, USA). Reactions containing DNA from known (100, 10, 1 and 0.1) *Bd* zoospore equivalent (ZE) standards were prepared, as well as controls with no DNA template. The mean concentration of the test samples was interpolated from the *Bd* standard curve and results were log+1 transformed to normalize data. All results are expressed as log(ZE+1).

Frogs were monitored daily for pathological or behavioural symptoms of chytridiomycosis, including lethargy, loss of appetite,

abnormal posture, areas of sloughed skin not fully removed or visible within the enclosure, loss of righting reflex, discoloured or reddened skin, and weight loss. Only frogs that exhibited these signs of infection were consequently used for tissue sampling. Frogs were swabbed immediately prior to euthanizing to determine the zoospore load (in zoospore equivalents) at the time of tissue sampling.

### Tissue sampling

Frogs were anaesthetized with an intraperitoneal injection of 60 mg kg<sup>-1</sup> thiopentone (Thiobarb Powder, Jurox Ltd, Rutherford, NSW, Australia) and killed by double-pithing. Ventral skin samples (<1 cm<sup>2</sup>) from the lower abdominal region were collected. Skin samples for immunohistochemistry were fixed in 10% neutral buffered formalin at 4°C overnight, after which formalin was replaced with 70% ethanol and samples were stored at 4°C until use. Skin samples for western blotting were frozen at -80°C until use and skin samples for RNA extraction were stored in RNA-later (Ambion Inc., Austin, TX, USA).

### Permeability assays

A Franz cell was used to measure the flux of 4 kDa FITC-dextran (FD-4; a fluorescent marker that travels solely through the paracellular pathway) across the skin (Fig. 2A). Ventral skin was collected from control ( $n=7$ ) and infected ( $n=10$ ) *L. caerulea* and immediately mounted epidermal side up onto the basolateral chamber of a Franz cell. The apical chamber contained 1 ml of 26 mmol l<sup>-1</sup> NaCl and the basolateral chamber contained 5 ml of Ringer's solution (in mmol l<sup>-1</sup>: 112 NaCl, 2.5 KCl, 10 D-glucose, 2 Na<sub>2</sub>HPO<sub>4</sub>, 1 CaCl<sub>2</sub>, 1 MgCl<sub>2</sub>, 5 Hepes sodium salt, pH 7.3–7.4 with an osmolality of 230±20 mOsm l<sup>-1</sup>). To examine the integrity of the paracellular pathway, 0.5 mg ml<sup>-1</sup> FD-4 was added to the basolateral chamber of the Franz cell and its appearance in the apical chamber was monitored. The basolateral solution was mixed continuously with a magnetic stirrer at 600 rpm. Aliquots (0.25 ml) of both the apical and basolateral solutions were collected immediately and again after 24 h. Sample fluorescence was analysed using a fluorescent plate reader (DTX880 Multimode Detector, Beckman Coulter Pty Ltd, Lane Cove West, NSW, Australia). The permeability ( $P$ ; cm s<sup>-1</sup>) of the skin samples was calculated using a modified equation from Kelly and Wood (2001):

$$P = \frac{\Delta F_{Ap} \times V_{Ap}}{F_{Bl} \times t \times A}, \quad (1)$$

where  $\Delta F_{Ap}$  is the change in fluorescence on the apical side,  $V_{Ap}$  is the volume of the apical chamber (1 ml),  $F_{Bl}$  is the fluorescence on the basolateral side,  $t$  is the total flux period (in s) and  $A$  defines the area of the Franz cell chamber opening (0.2 cm<sup>2</sup>).

### RNA extraction and cDNA synthesis

Skin samples were homogenized using a TissueLyser II (Qiagen). Total RNA was isolated using an RNeasy Mini kit (Qiagen) as per the manufacturer's instructions. RNA purity (absorbance at 260 nm/280 nm) was assayed by spectrometry, and RNA concentration was quantified using a Qubit fluorometer (ThermoFisher Scientific, Waltham, MA, USA). RNA was then reverse transcribed into cDNA using the QuantiTech Reverse Transcription Kit (Qiagen) according to the manufacturer's instructions.

### Analysis of TJ protein mRNA by PCR and qPCR

For PCR, the Taq PCR Master Mix Kit (Qiagen) was used. The following reaction conditions were utilized: 1 cycle of initial denaturation (95°C, 10 min), then 40 cycles of denaturation

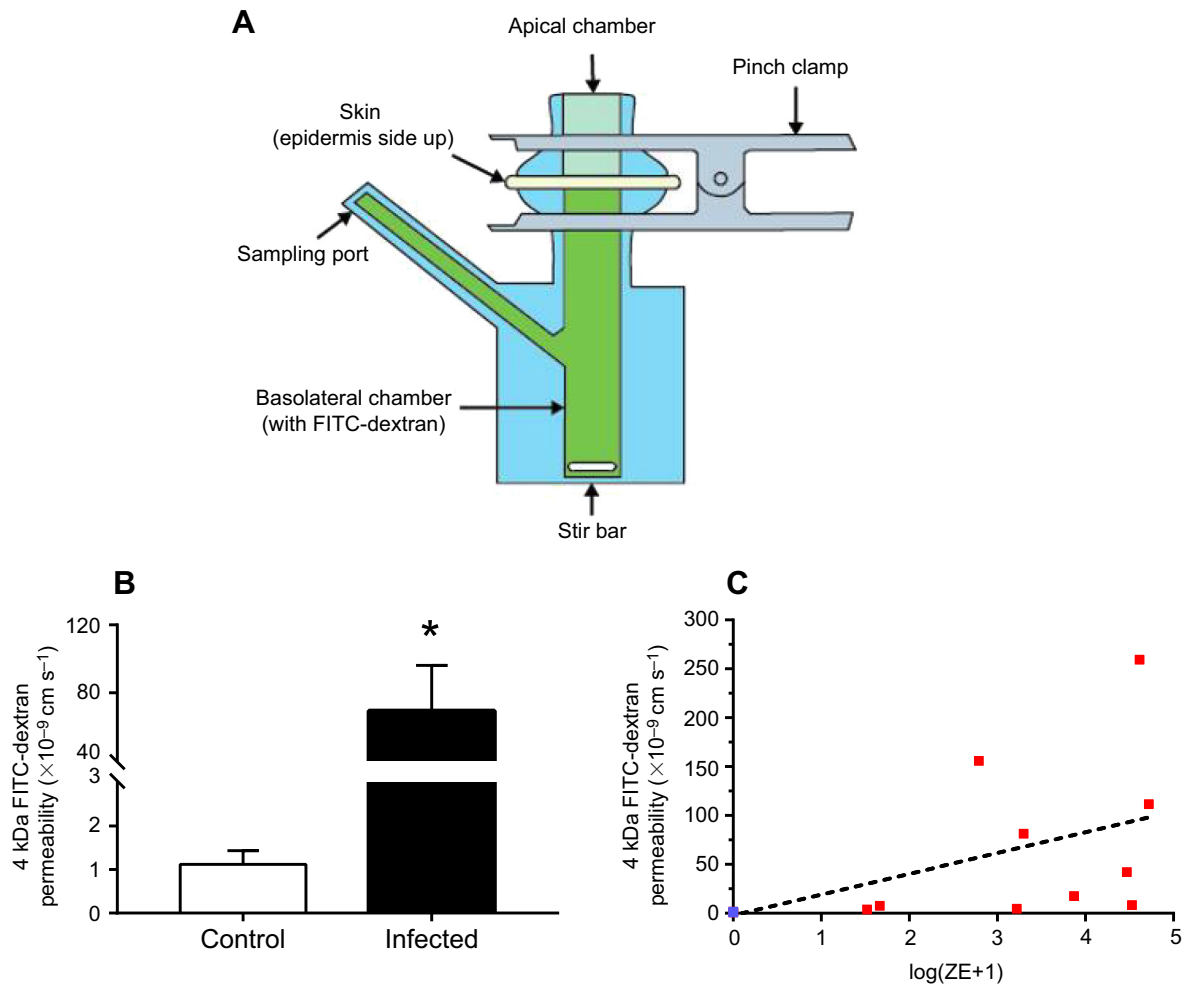


**Fig. 2. Permeability of 4 kDa FITC-dextran (FD-4) through the skin of control and *Bd*-infected *Litoria caerulea*.** (A) Schematic diagram of a Franz cell setup, with the skin held between two chambers. (B) The mean ( $\pm$ s.e.m.) paracellular permeability of FD-4 through control ( $n=7$ ) and infected ( $n=10$ ) frog skin. Asterisks indicate a significant difference between control and infected frogs as determined by a Mann–Whitney *U*-test ( $P \leq 0.001$ ). (C) Individual permeability values of control (blue) and infected (red) animals plotted against  $\log[\text{zoospore equivalents (ZE)}+1]$ . Frogs were swabbed immediately prior to the permeability assays to determine the zoospore equivalents.

(95°C, 30 s), annealing (56–60°C, 30 s) and extension (72°C, 30 s), followed by a final single extension cycle (72°C, 5 min). PCR-generated amplicons were visualized by agarose gel electrophoresis (1.5%, 120 V separation for 1 h).

Gene-specific primers were designed for *L. caerulea* (Table 1) using the transcriptome of a closely related species (*Pseudacris regilla*). Primers were confirmed to produce single bands on an agarose gel, the amplicon was sequenced, and primers that did not have 100% sequence homology were re-synthesized to be specific to *L. caerulea* genes. TJ protein mRNA abundance was examined by qPCR using a Mini Opticon real-time PCR detection system (MJ Mini Cycler, Bio-Rad Laboratories, Inc.) and PowerSYBR Supermix (Applied Biosystems) under the following conditions: one initial cycle of denaturation (95°C, 10 min), followed by 40 cycles of denaturation (95°C, 30 s), annealing (58–61°C, 15 s) and extension (60°C, 45 s). A melting curve was constructed after each qPCR run, ensuring that a single product was synthesized during each reaction. For all qPCR analyses, transcript abundance was normalized to *ef-1 $\alpha$*  transcript abundance after determining by statistical analysis that it did not significantly alter ( $P=0.413$ ) in response to *Bd* infection. *Litoria*

*caerulea ef-1 $\alpha$*  mRNA was amplified using primers reported in Table 1.

#### Antibodies

The affinity purified polyclonal antibodies used for western blot and immunohistochemistry analysis were raised against human Cldn-1 (ThermoFisher Scientific 519000), Oc1n (ThermoFisher Scientific 711500) and Tric (EMD Millipore AB2980).

#### Immunohistochemical analysis

Fixed skin samples were dehydrated and embedded in paraffin wax. Transverse sections (6  $\mu\text{m}$ ) of control and infected ventral skin were cut on a rotary microtome (RM2245, Leica Microsystems, Nussloch, Germany) and mounted on glass slides. Additionally, sections along the frontal plane of the skin were obtained to visualize the punctate Tric staining that would be difficult to observe in transverse sections. Sections on slides were first dewaxed in xylene, followed by rehydration using a graded ethanol series. Subsequently, slides were washed for 10 min in different PBS solutions: 1% Tween-20 (PBS-T), then in 0.05% Triton X-100 in PBS (PBS-TX), and finally in 10% antibody dilution buffer (ADB;

**Table 1. Primer sets, PCR annealing temperatures ( $T_a$ ), amplicon sizes and gene accession numbers for *Litoria caerulea* tight junction (TJ) proteins and elongation factor-1 $\alpha$** 

TJ protein	Gene	Primers	$T_a$	Amplicon size (bp)	Accession no.
Elongation factor-1 $\alpha$	<i>ef-1<math>\alpha</math></i>	F: GGCAAGTCCACAACAACC R: GTCCAGGGGCATCAATAA	56	229	MH660750
Claudin-1	<i>cldn-1</i>	F: GGCTTGATAGGGTGGATTG R: ACCTTGGCCTTCATCACCTC	60	316	MH660751
Claudin-4	<i>cldn-4</i>	F: TGCCTTCATCGGTAACAACA R: AACTCCCAGGATAGCCACAA	60	187	MH660752
Occludin	<i>ocln</i>	F: TGCTATTGTTCTGGGGTTCC R: CTTCTCGTTGTATTGCGACA	60	218	MH660753
Tricellulin	<i>tric</i>	F: TAAGCGGATACATTCCAGCA R: CAGCGTTCCTTTTCTCCAA	60	316	MH660754
Zonula occludens-1	<i>zo-1</i>	F: GGGATGAGCGAGCAACTCTA R: GCACCAGGCTTTGACACTC	60	265	MH660755

2% goat serum, 1% BSA, 0.1% cold fish skin gelatin, 0.1% Triton X-100, 0.05% Tween-20, 0.01 mol l<sup>-1</sup> PBS) in PBS. Sections were incubated with rabbit polyclonal anti-TJ protein antibodies (1:100 dilution: 2.5  $\mu$ g ml<sup>-1</sup> of Cldn-1 and Ocln, 1  $\mu$ g ml<sup>-1</sup> of Tric) overnight at room temperature (RT). Slides were then rinsed in PBS-T and incubated with Texas Red (TR)-labelled goat anti-rabbit antibody (1:500 in ADB; SC2780, Santa-Cruz Biotechnology, Santa Cruz, CA, USA) for 1 h at RT. Slides were rinsed and mounted with coverslips using Fluoroshield™ DAPI Mounting Medium (Sigma-Aldrich, Sydney, NSW, Australia). Fluorescence images were captured using a Leica DMi8 Inverted Confocal microscope and merged using ImageJ software.

#### Western blot analysis

Frozen skin samples were homogenized using a TissueLyser II (Qiagen) in chilled radioimmunoprecipitation assay lysis buffer (RIPA; 0.6% Tris-HCl, 0.8% NaCl, 1% deoxycholic acid, 1% Triton X-100, 1% SDS, 1 mmol l<sup>-1</sup> EDTA, 1 mmol l<sup>-1</sup> PMSF and 1 mmol l<sup>-1</sup> DTT) containing 1:20 protease inhibitor cocktail (Sigma-Aldrich). Protein content was quantified using Bradford reagent (Sigma-Aldrich) according to the manufacturer's guidelines. Skin protein (25  $\mu$ g) was electrophoretically separated with NuPAGE™ 10% Bis-Tris protein gels and transferred to polyvinylidene difluoride (PVDF) membranes (Immobilon-P PVDF Membrane, Merck, Sydney, NSW, Australia). Following transfer, the membrane was washed in Tris-buffered saline with Tween-20 [TBS-T; TBS (10 mmol l<sup>-1</sup> Tris, 150 mmol l<sup>-1</sup> NaCl, pH 7.4) with 0.05% Tween-20], and blocked for 1 h at RT in 5% non-fat dried skimmed milk powder in TBS-T (5% milk TBS-T). The membrane was then incubated overnight at 4°C with rabbit polyclonal anti-TJ protein antibodies (1:1000 dilution in 5% milk TBS-T). Membranes were incubated with a horseradish peroxidase (HRP)-conjugated goat anti-rabbit secondary antibody (1:5000 in 5% milk TBS-T) for 1 h at RT. Then, blots were incubated in 1-Step Ultra TMB Blotting Substrate Solution (ThermoFisher Scientific) for 1–15 min at RT and scanned. Following imaging, membranes were incubated with Coomassie Brilliant Blue R-250 staining solution as a modified protocol of that outlined in Welinder and Ekblad (2010) to quantify total protein. Coomassie staining solution was combined with 5% MeOH and membranes were stained for ~5 min. Membranes were then destained in acetic acid/ethanol/water (1:5:4 ratio), rinsed in water and scanned. TJ protein and total protein abundance were quantified using ImageJ software. Total protein abundance was used for normalizing TJ protein abundance after statistically validating that it did not significantly differ between control and experimental groups.

#### Statistical analyses

All data are expressed as means  $\pm$  s.e.m. ( $n$ ), where  $n$  represents the number of frogs sampled, or as individual data points depending on the nature of the data. Differences between mean skin permeability data were analysed using the Mann–Whitney  $U$ -test and a linear regression was fitted to individual data points. All other significant differences ( $P \leq 0.05$ ) between groups were determined using Student's  $t$ -test. All statistical analyses were performed using SigmaPlot 12.5 (Systat Software Inc., San Jose, CA, USA) or in RStudio 1.0.136 (R Studio Team 2016).

## RESULTS

#### Permeability of FITC-dextran (FD-4) through the skin of *Bd*-infected *L. caerulea*

There was little FD-4 permeability through the skin of control frogs after 24 h (Fig. 2B). *Bd* infection had a significant effect on skin paracellular permeability to FD-4 ( $P < 0.001$ ), and the skin of infected animals was on average 62 times more permeable than the skin of control animals. Additionally, the paracellular permeability increased significantly with infection intensity ( $P = 0.0149$ ,  $R^2 = 0.3354$ ; Fig. 2C).

#### Effect of *Bd* infection on TJ protein mRNA abundance in the ventral skin of *L. caerulea*

The abundance of *cldn-1*, *cldn-4*, *ocln*, *tric* and *zo-1* transcripts was examined in the skin of green tree frogs. The most highly expressed gene in the skin was *cldn-1* (Fig. 3). With *Bd* infection, the abundance of *cldn-1*, *cldn-4*, *ocln*, *tric* and *zo-1* increased 2- to 3-fold (Fig. 4).

#### Effect of *Bd* infection on Cldn-1 in the skin of *L. caerulea*

Cldn-1 immunofluorescence was localized to the epidermis of control frogs and exhibited peri-junctional staining from the basal to the upper regions of the epidermis (Fig. 5A). With *Bd* infection, Cldn-1 fluorescence decreased in the epidermis (Fig. 5B). On a western blot, the Cldn-1 antibody detected one band of approximately 22 kDa (Fig. 5C), and Cldn-1 protein abundance significantly decreased in infected frogs compared with control frogs (Fig. 5D). In addition to decreased Cldn-1 fluorescence, the epidermis of infected frogs also appeared thinner than in control animals (Figs 5B and 6B).

#### Effect of *Bd* infection on Ocln in the skin of *L. caerulea*

Ocln localized to the basal epidermal layer of control animals (Fig. 6A). Ocln immunofluorescence could also be seen lining glands in the dermis. Following *Bd* infection, there was no

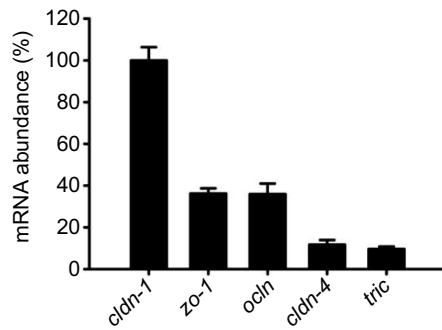


**Fig. 3. Transcript abundance of claudin (*cldn*)-1, *cldn*-4, occludin (*ocln*), tricellulin (*tric*) and zonula occludens-1 (*zo-1*) in the ventral skin of control *L. caerulea*.** Relative transcript abundance of TJ proteins in healthy frogs was examined by qPCR. The mRNA abundance of *cldn-1* was set to 100% and all other transcripts were compared with it. Data are expressed as means  $\pm$  s.e.m. ( $n=8$ ). In order to normalize mRNA abundance, *ef-1 $\alpha$*  was used as the reference gene.

qualitative decrease in Ocln fluorescence in the epidermis (Fig. 6B) and around dermal glands (not shown). Western blotting revealed one band of approximately 62 kDa (Fig. 6C), and there was no significant decrease in Ocln abundance with *Bd* infection (Fig. 6D).

#### Effect of *Bd* infection on Tric in the skin of *L. caerulea*

Frontal sections of the skin were taken to visualize Tric staining in the epidermis, and localization was found to be punctate at regions where more than two cells interfaced (Fig. 7A). In *Bd*-infected animals, Tric fluorescence increased and localized to areas where the epidermal cells appeared to be dissociating from one another (Fig. 7B white lines, Fig. 7D). Western blotting revealed one band of ~55 kDa (Fig. 7E) and Tric abundance was found to significantly increase with *Bd* infection (Fig. 7F).

## DISCUSSION

### Overview

This study examined the effects of *Bd* infection on the paracellular permeability of amphibian skin and the associated changes in TJ protein abundance. It was found that *Bd* infection resulted in an increase in paracellular permeability of the skin. In addition, changes in TJ protein and transcript abundance as well as immunohistochemical observations of bicellular and tricellular TJ proteins suggests that alterations in paracellular permeability arose in association with a perturbation of the epidermal TJ complex. This indicates that dysregulation of the TJ complex may contribute to the compromised skin barrier function of *L. caerulea* infected with *Bd*. Together, these data support the contention that *Bd* infection directly compromises the amphibian epidermal TJ complex and paracellular permeability, which contribute, at least in part, to previously reported *Bd*-induced disturbances in amphibian salt and water balance (Voyles et al., 2007, 2009; Wu et al., 2018). Additionally, our detailed study of TJ proteins in amphibian skin provides new insights into how cutaneous paracellular permeability is regulated.

#### *Bd* infection increases the paracellular permeability of *L. caerulea* skin

The paracellular permeability of the skin increased significantly with *Bd* infection (Fig. 2B,C). This is consistent with earlier studies showing that *Bd* decreased TER across *L. caerulea* skin, leading to a disruption of ionic and osmotic homeostasis (Voyles et al., 2009). Therefore, the previously reported decrease in TER and disrupted

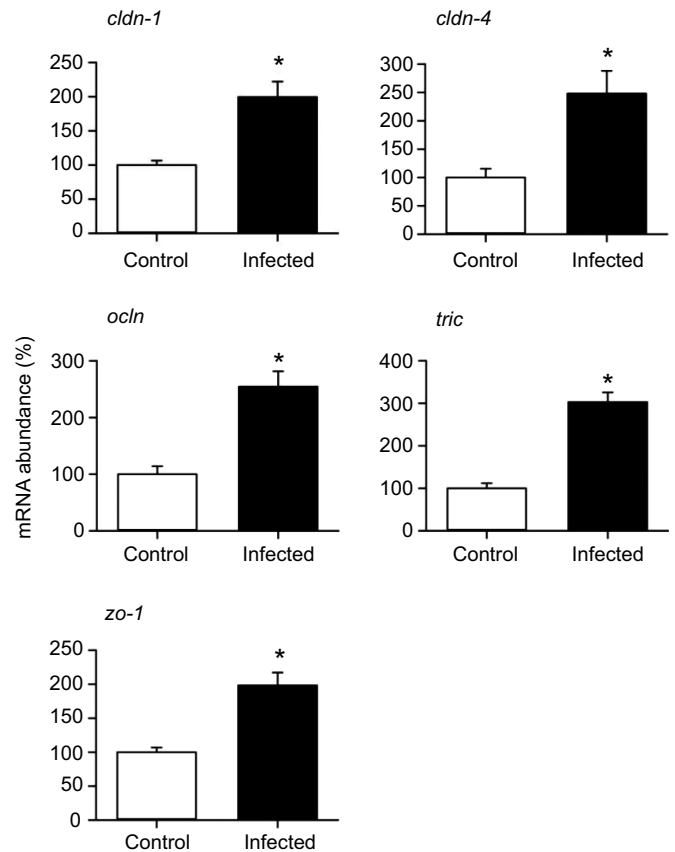


**Fig. 4. Effect of *Bd* infection on *cldn*-1, *cldn*-4, *ocln*, *tric* and *zo-1* mRNA abundance in the ventral skin of *L. caerulea*.** Transcript abundance of TJ proteins in infected frog skin was expressed relative to abundance in control animals assigned a value of 100%. All data are expressed as means  $\pm$  s.e.m. ( $n=8$ ). Asterisks indicate a significant difference between control and infected frogs as determined by Student's *t*-test ( $P \leq 0.05$ ). *ef-1 $\alpha$*  was used as a reference gene.

osmoregulatory capacity may have been due, at least in part, to a loss of the paracellular barrier of infected skin.

The effects of *Bd* on skin permeability were dependent on infection load, with increasing *Bd* loads increasing the permeability of the skin. Previous studies using cultured intestinal Caco-2 epithelia and cultured human epidermal keratinocytes demonstrated that purified fungal toxins increased paracellular permeability in a dose-dependent manner (Watanabe et al., 1999; McLaughlin et al., 2004, 2009; Yuki et al., 2007). This may suggest that the increased paracellular permeability observed in *Bd*-infected frogs in the current study could be due, at least in part, to toxins released by *Bd*. However, there is additional evidence implicating other pathogenic factors in this process. For example, exposure of *Xenopus laevis* skin to supernatant containing proteases produced by *Bd* resulted in the disruption of adherens junction components in the skin (Brutyn et al., 2012). Therefore, it is plausible that the same proteases produced by *Bd* can also influence TJs and may have contributed to the infection load-dependent increase in paracellular permeability of the skin observed in the current study.

#### Effect of *Bd* infection on Cldn-1, Ocln and Tric abundance

The localization and abundance of Cldn-1, Ocln and Tric were examined to determine whether the *Bd* infection-induced increase in skin paracellular permeability was linked to the molecular machinery of the TJ. Various infectious agents have been known to target

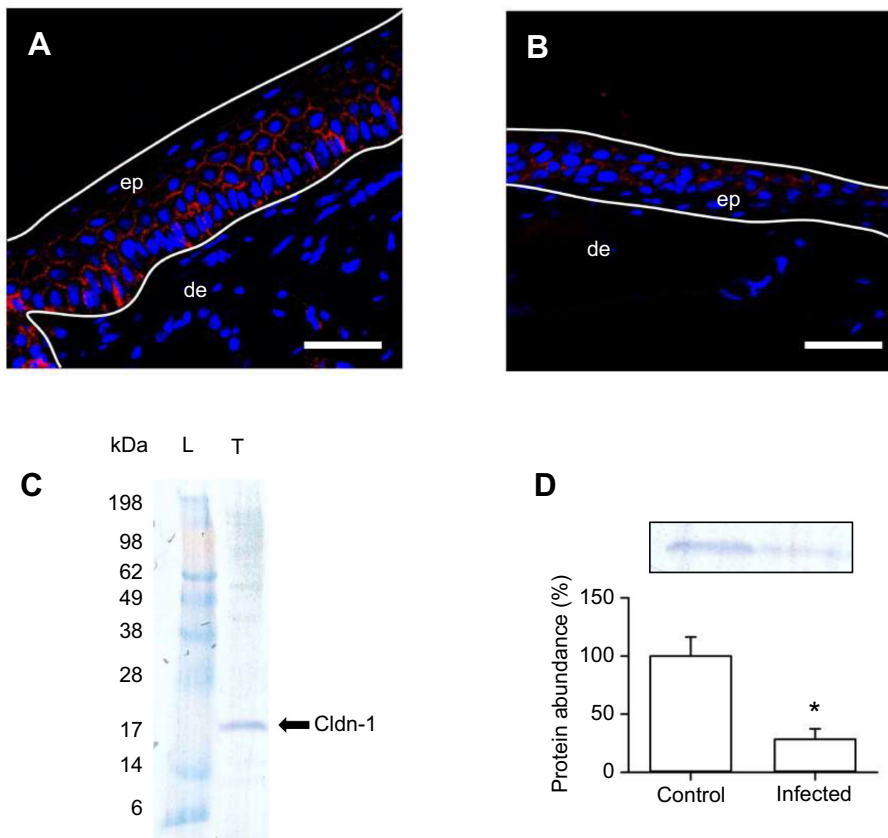


**Fig. 5. Effect of *Bd* infection on the localization and abundance of Cldn-1 in the ventral skin of *L. caerulea*.** (A,B) Localization of Cldn-1 (red) in the skin of (A) control and (B) infected frogs. ep, epidermis; de, dermis. Nuclear staining is in blue. Scale bars: 20 μm. (C) Representative western blot of Cldn-1 in the skin. L, ladder; T, total protein fraction. (D) Effect of *Bd* on Cldn-1 abundance. Protein abundance of Cldn-1 in infected frog (means±s.e.m.) is expressed relative to abundance in control animals, assigned a value of 100% after normalization using total protein ( $n=7$ ). Asterisks indicate a significant difference between control and infected treatments as determined by Student's *t*-test ( $P<0.05$ ). A representative western blot is shown above the graph.

specific TJ proteins in order to disrupt the epithelial barrier and spread within the infected tissue. Notable examples are *Clostridium perfringens* targeting Cldn-3 and Cldn-4 proteins in the human intestine (Katahira et al., 1997; Fujita et al., 2000; Robertson et al., 2010), and *Shigella flexneri* targeting Tric in cultured Madin–Darby canine kidney cells (Fukumatsu et al., 2012). Additionally, fungal toxins have been found to selectively alter the abundance of specific TJ proteins such as Cldn-1, Cldn-4, Ocln and ZO-1 in cultured Caco-2 cells and human epidermal keratinocytes in conjunction with increased FD-4 permeability (McLaughlin et al., 2004, 2009; Yuki et al., 2007). Therefore, because the paracellular pathway is regulated by the TJ complex, the observed loss of skin barrier properties in this study following *Bd* infection (Fig. 2) may be linked, at least in part, to an altered abundance of TJ proteins.

Cldn-1, Ocln and Tric proteins immunolocalized to the epidermis of *L. caerulea*, which directly interfaces with the external environment. Therefore, alterations in the abundance of these TJ proteins are likely to have impacted the paracellular permeability of the skin. In addition to alterations in protein abundance, the epidermis of infected animals appeared thinner, which is in accordance with previous observations (Berger et al., 2005; Greenspan et al., 2012). This may have also contributed to the increased paracellular permeability of the skin because there were fewer cell layers that could express TJ proteins and act as barriers to solute movement.

The most abundant TJ protein transcript examined was *cldn-1* (Fig. 3). Cldn-1 has previously been shown to be indispensable for the barrier function of mammalian skin, where mutations in this protein resulted in multiple skin defects and increased epidermal paracellular permeability (Hadj-Rabia et al., 2004; Brandner, 2009; Kirschner et al., 2009; De Benedetto et al., 2011; Günzel and Yu, 2013; Kirchmeier et al., 2014; Tokumasu et al., 2017). Cldn-1-

deficient mice died shortly after birth as a result of evaporative water loss through the skin, implying that Cldn-1 may act as a water barrier in mammalian skin (Furuse et al., 2002). Additionally, Cldn-1 has been shown to be important in cutaneous wound healing in humans (Volksdorf et al., 2017). To date, no work has been conducted on Cldn-1 in the skin of amphibians; however, Cldn-1 has been shown to respond to changes in ion concentration and osmolarity in renal epithelial cells of *Xenopus* (Tokuda et al., 2010). Therefore, Cldn-1 in the skin of *L. caerulea* is likely to be important for maintaining skin barrier properties.

Cldn-1 protein abundance decreased with *Bd* infection (Fig. 5D). Given that Cldn-1 is highly abundant in the skin of *L. caerulea*, the decrease in Cldn-1 protein abundance alone may have contributed heavily to the observed disruption of the skin barrier properties. Despite the decrease in Cldn-1 protein abundance following *Bd* infection, there was an increase in *cldn-1* mRNA levels (Fig. 4). This may indicate that *cldn-1* mRNA was not being translated. Previous reports have found that the abundance of various proteins, including TJ proteins, did not match mRNA abundance because the transcripts were post-transcriptionally or post-translationally modified (Takahashi et al., 2009; Fujii et al., 2016; Liu et al., 2016). Therefore, it is possible that, in the current study, the infection resulted in post-transcriptional or post-translational modifications of Cldn-1, lowering Cldn-1 protein levels. Alternatively, the decrease in Cldn-1 protein abundance may have been caused by degradation of Cldn-1 by proteases that were previously reported to be produced by *Bd* (Brutyn et al., 2012) or the direct effect of fungal toxins.

The abundance of the other bTJ protein, Ocln, did not change following *Bd* infection (Fig. 6D). Ocln is regarded to be an important TJ protein in epithelial barriers (Yu et al., 2005). In *Xenopus*, Ocln

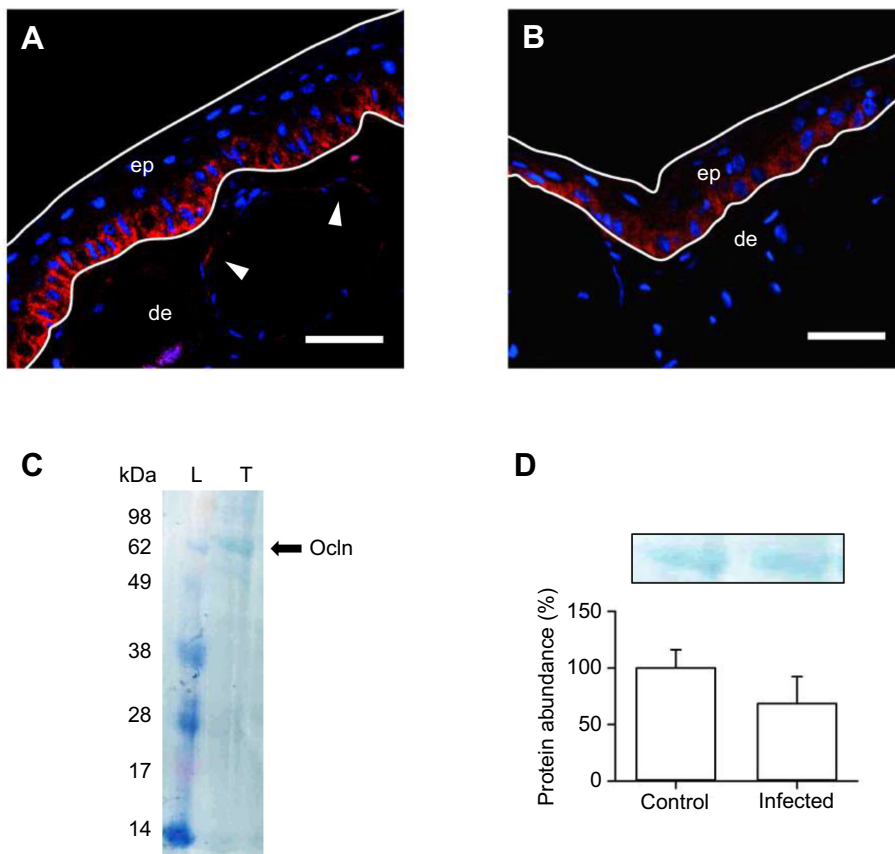


**Fig. 6. Effect of *Bd* infection on the localization and abundance of Ocln in the ventral skin of *L. caerulea*.** (A,B) Localization of Ocln (red) in the skin of (A) control and (B) infected frogs. Arrowheads point to Ocln fluorescence around dermal glands. ep, epidermis; de, dermis. Nuclear staining is in blue. Scale bars: 20 µm. (C) Representative western blot of Ocln in the skin. L, ladder; T, total protein fraction. (D) Effect of *Bd* on Ocln abundance. Protein abundance of Ocln in infected frog skin (means ± s.e.m.) is expressed relative to abundance in control animals, assigned a value of 100% after normalization using total protein ( $n=7$ ). A representative western blot is shown above the graph.

has been shown to exhibit spatial differences in tissue localization that relate to the resistance of epithelia, as well as organ-specific alterations in abundance following changes in the salt content of their surroundings (Chasiotis and Kelly, 2009). Additionally, Ocln is known to undergo post-transcriptional/translational modifications in vertebrates, which remove it from the TJ complex (reviewed in Cummins, 2012). Therefore, in the current study, because *ocln* mRNA abundance increased with infection (Fig. 4) but Ocln protein abundance did not, it may have been post-translationally modified or degraded as a result of *Bd* infection.

Finally, Tric protein levels increased following *Bd* infection (Fig. 7F). Tric is known to be a barrier-forming protein in multiple vertebrates (Günzel and Fromm, 2012; Kolosov and Kelly, 2013, 2018) and is concentrated at the tTJ between adjacent epithelial cells, which runs in a basal-to-apical direction, in a plane perpendicular to the bTJ (Ikenouchi et al., 2005). Given its localization, Tric belongs to a different junctional structure and may in part be regulated by different regulatory networks from those of its bTJ counterparts (e.g. Masuda et al., 2010; Krug et al., 2018; reviewed in Mariano et al., 2011). This could explain why there was an increase in Tric protein abundance, whereas Cldn-1 and Ocln protein levels did not increase. The upregulated Tric protein abundance may have been a by-product of the increase in *tric* mRNA abundance (Fig. 4). Tric protein abundance may have increased to compensate for the loss of paracellular barrier properties that occurred with *Bd* infection. In line with this idea, Tric fluorescence increased around areas where the infected epidermis was disrupted. Previous studies demonstrated that during epithelial maturation and establishment of resistive properties, Tric is first shuttled to the bTJ (Krug et al., 2009). Following this, after the tricellular contact points are defined, Tric is

incorporated into the tTJ (Krug et al., 2009). Therefore, in the current study Tric may be participating in the healing of *Bd* infection-induced epidermal wounds, aimed at re-establishing paracellular barrier properties.

#### All examined TJ protein transcripts increase in abundance with *Bd* infection

In addition to Cldn-1, Ocln and Tric mRNA and protein abundance, the effect of *Bd* infection on *cldn-4* and *zo-1* transcript abundance was also examined. ZO-1 is a cytosolic scaffolding protein (Gonzalez-Mariscal et al., 2003) and Cldn-4 is a bTJ protein, the properties of which depend on the tissue and type of associated Cldn proteins (Günzel and Fromm, 2012). Fungal toxins have been known to alter Cldn-4 and ZO-1 protein abundance in Caco-2 cells (McLaughlin et al., 2009); therefore it is possible that *Bd* infection may alter the abundance of these proteins as well. In the current study, the abundance of *cldn-4* and *zo-1* increased with *Bd* infection (Fig. 4). One potential explanation is that increased *cldn-4* and *zo-1* abundance reflects an attempt to increase protein levels and enhance barrier function in the compromised skin of *Bd*-infected frogs. Alternatively, because all of the examined TJ protein transcripts increased in abundance, this could reflect a tissue response to a systemic stress-induced factor released during *Bd* infection. For example, corticosterone levels are reported to rise during stress and inflammatory responses in amphibians (Rollins-Smith, 2017), and specifically in *L. caerulea* infected with *Bd* (Peterson et al., 2013). Corticosteroids have been shown to alter mRNA and protein abundance of Ocln (Chasiotis and Kelly, 2011; Förster et al., 2005), Tric (Kolosov and Kelly, 2013), Cldns (Kielgast et al., 2016; Kobayashi et al., 2016; Gauberg et al., 2017; Kolosov and Kelly, 2017; Kolosov et al., 2017b) and ZO-1 (Singer et al., 1994;

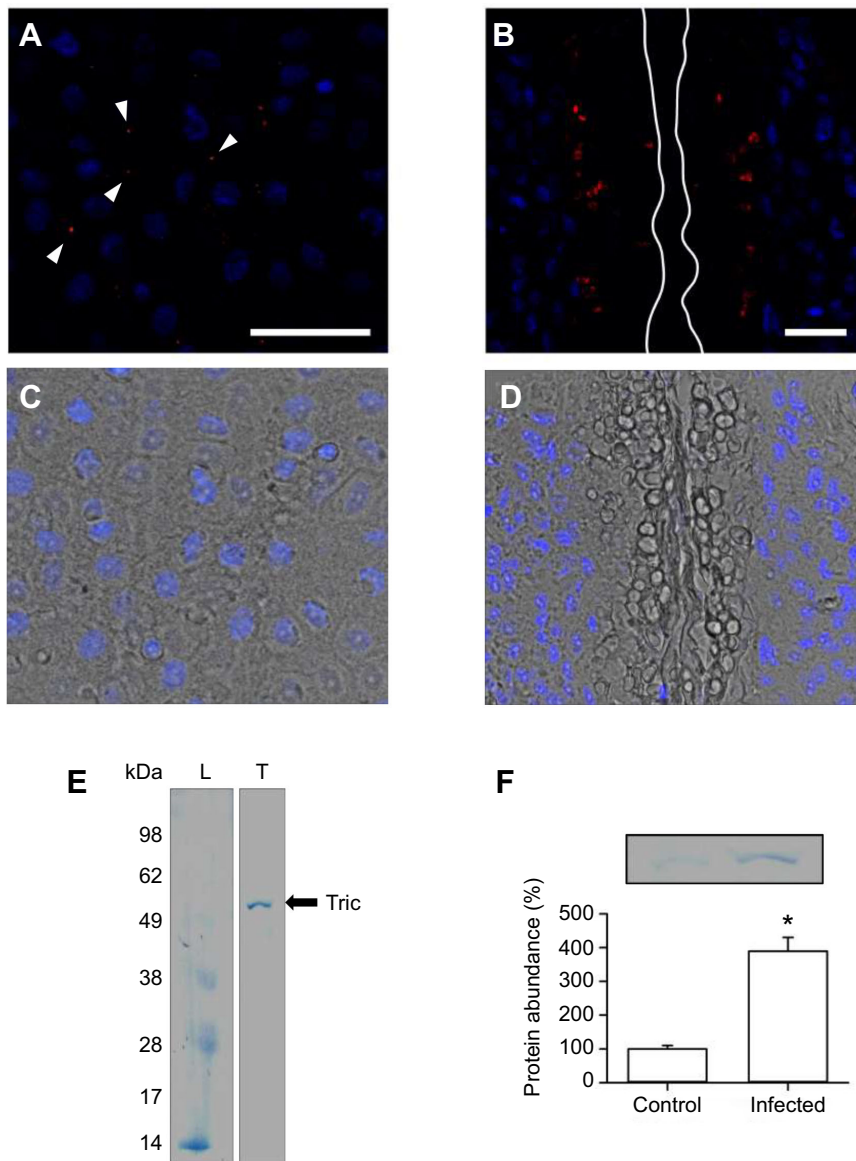


**Fig. 7. Effect of *Bd* infection on the localization and abundance of Tric in the epidermis of *L. caerulea*.** (A–D) A top-down view of the epidermis. The localization of Tric (red) in the skin of (A) control and (B) infected frogs is shown. Arrowheads point to Tric staining between three cells and white lines illustrate disrupted epidermal margins. Nuclear staining is in blue. Scale bars: 20  $\mu$ m. C and D depict nuclear staining with brightfield image overlay. (E) Representative western blot of Tric in the skin. L, ladder; T, total protein fraction. (F) Effect of *Bd* on Tric abundance. Protein abundance of Tric in infected frog skin (means  $\pm$  s.e.m.) is expressed relative to abundance in control animals, assigned a value of 100% after normalization using total protein ( $n=6$ ). Asterisks indicate a significant difference between control and infected treatments as determined by Student's *t*-test ( $P \leq 0.05$ ). A representative western blot is shown above the graph.

Chasiotis and Kelly, 2011) in various vertebrate models. Therefore, increased systemic levels of corticosterone in *L. caerulea* that would occur with infection may have triggered an *en masse* increase in TJ protein transcript abundance.

### Conclusions and significance

This study directly demonstrates that the paracellular barrier is compromised in the epidermis of amphibians infected with *Bd*. This supports the notion that the paracellular pathway is an important barrier to solute movement across the skin of healthy frogs. Therefore, disruption of the skin barrier properties, such as paracellular permeability, can lead to the loss of osmoregulatory homeostasis in amphibians.

Increased paracellular permeability is correlated with *Bd* infection load and *Bd* infection results in a uniform increase in the abundance of all TJ-related transcripts examined in this study. However, at the protein level, *Bd* infection may target specific bTJ proteins, while the tTJ may not be directly targeted. Importantly, a decrease in abundance of a prominent epidermal Cldn in vertebrates, Cldn-1, may contribute significantly to the observed loss of barrier properties. Overall, TJ proteins in the skin of

amphibians are probably differentially regulated, and their dysregulation results in the loss of skin barrier properties.

Presently, the deleterious effects of *Bd* infection are broadly accepted but not completely understood, and the current data provide new insight into mechanisms of chytrid fungus action on the skin of amphibians. Future comparative studies examining the effect of *Bd* on TJ proteins in susceptible and resistant animals would be useful for understanding which TJ proteins are impacted by *Bd* infection. It is plausible that frogs with greater resistance to *Bd* may have a larger repertoire of TJ proteins that are not affected by *Bd* infection. Additionally, *in vitro* studies that express select TJ proteins in heterologous systems should be conducted to determine whether *Bd* is able to directly affect the expression or degradation of these proteins. Given the devastating effects of *Bd* on amphibian populations worldwide (Berger et al., 2005; Fisher et al., 2009; Kilpatrick et al., 2010), understanding its interaction with TJ proteins in the skin will be important for elucidating the mechanism of skin barrier disruption and species susceptibility to *Bd* infection. More generally, examining the fungal–TJ interaction in vertebrate epithelia will allow us to gain insight into mechanisms of fungal pathogenicity that were previously unexplored.

## Acknowledgements

The authors would like thank Dr Gary Sweeney (Department of Biology, York University) for the contribution of antibodies.

## Competing interests

The authors declare no competing or financial interests.

## Author contributions

Conceptualization: J.G., S.P.K., C.E.F.; Methodology: J.G., N.W., R.L.C., S.P.K., C.E.F.; Validation: J.G.; Formal analysis: J.G., R.L.C.; Investigation: J.G., N.W., R.L.C.; Resources: S.P.K., C.E.F.; Writing - original draft: J.G.; Writing - review & editing: J.G., N.W., R.L.C., S.P.K., C.E.F.; Visualization: J.G.; Supervision: S.P.K., C.E.F.; Funding acquisition: J.G., S.P.K., C.E.F.

## Funding

This work was supported by a Natural Sciences and Engineering Research Council of Canada (NSERC) Discovery Grant [S.P.K.], an Australia Research Council Discovery Grant [C.E.F.], as well as a Natural Sciences and Engineering Research Council of Canada Graduate Scholarship [J.G.], a Natural Sciences and Engineering Research Council of Canada Michael Smith Foreign Study Supplement [J.G.], a Company of Biologists Travel Fund [J.G.], and a Canadian Society of Zoologists Integrative Ecology and Evolution Student Research Grant [J.G.].

## References

- Baltzegar, D. A., Reading, B. J., Brune, E. S. and Borski, R. J. (2013). Phylogenetic revision of the claudin gene family. *Mar. Genomics*, **11**, 17–26.
- Berger, L., Speare, R. and Skerratt, L. F. (2005). Distribution of *Batrachochytrium dendrobatidis* and pathology in the skin of green tree frogs *Litoria caerulea* with severe chytridiomycosis. *Dis. Aquat. Organ.* **68**, 65–70.
- Bouhet, S. and Oswald, I. P. (2005). The effects of mycotoxins, fungal food contaminants, on the intestinal epithelial cell-derived innate immune response. *Vet. Immunol. Immunopathol.* **108**, 199–209.
- Boutillier, R. G., Stiffler, D. F. and Toews, D. P. (1992). Exchange of respiratory gases, ions, and water in amphibious and aquatic amphibians. In *Environmental Physiology of the Amphibians* (ed. M. E. Feder and W. Burggren), pp. 100–107. Chicago, USA: The University of Chicago Press.
- Boyle, D. G., Boyle, D. B., Olsen, V., Morgan, J. A. T. and Hyatt, A. D. (2004). Rapid quantitative detection of chytridiomycosis (*Batrachochytrium dendrobatidis*) in amphibian samples using real-time Taqman PCR assay. *Dis. Aquat. Organ.* **60**, 141–148.
- Brandner, J. M. (2009). Tight junctions and tight junction proteins in mammalian epidermis. *Eur. J. Pharm. Biopharm.* **72**, 289–294.
- Brutyn, M., D'Herde, K., Dhaenens, M., Van Rooij, P., Verbrugghe, E., Hyatt, A. D., Croubels, S., Deforce, D., Ducatelle, R., Haesebrouck, F. et al. (2012). *Batrachochytrium dendrobatidis* zoospore secretions rapidly disturb intercellular junctions in frog skin. *Fungal Genet. Biol.* **49**, 830–837.
- Bruus, K., Kristensen, P. and Larsen, E. H. (1976). Pathways for chloride and sodium transport across toad skin. *Acta Physiol. Scand.* **97**, 31–47.
- Campbell, C. R., Voyles, J., Cook, D. I. and Dinudom, A. (2012). Frog skin epithelium: Electrolyte transport and chytridiomycosis. *Int. J. Biochem. Cell Biol.* **44**, 431–434.
- Cardellini, P., Davanzo, G. and Citi, S. (1996). Tight junctions in early amphibian development: Detection of junctional cingulin from the 2-cell stage and its localization at the boundary of distinct membrane domains in dividing blastomeres in low calcium. *Dev. Dyn.* **207**, 104–113.
- Castillo, G. A., Coviello, A. and Orce, G. G. (1991). Effect of theophylline on the electrolyte permeability of the isolated skin of the toad *Bufo arenarum*. *Arch. Int. Physiol. Biochim. Biophys.* **99**, 257–264.
- Chang, D.-J., Hwang, Y.-S., Cha, S.-W., Chae, J.-P., Hwang, S.-H., Hahn, J.-H., Bae, Y. C., Lee, H.-S. and Park, M. J. (2010). Xclaudin 1 is required for the proper gastrulation in *Xenopus laevis*. *Biochem. Biophys. Res. Commun.* **397**, 75–81.
- Chapman, J. A., Kirkness, E. F., Simakov, O., Hampson, S. E., Mitros, T., Weinmaier, T., Rattei, T., Balasubramanian, P. G., Borman, J., Busam, D. et al. (2010). The dynamic genome of *Hydra*. *Nature* **464**, 592–596.
- Chasiotis, H. and Kelly, S. P. (2008). Occludin immunolocalization and protein expression in goldfish. *J. Exp. Biol.* **211**, 1524–1534.
- Chasiotis, H. and Kelly, S. P. (2009). Occludin and hydromineral balance in *Xenopus laevis*. *J. Exp. Biol.* **212**, 287–296.
- Chasiotis, H. and Kelly, S. P. (2011). Effect of cortisol on permeability and tight junction protein transcript abundance in primary cultured gill epithelia from stenohaline goldfish and euryhaline trout. *Gen. Comp. Endocrinol.* **172**, 494–504.
- Chasiotis, H., Kolosov, D., Bui, P. and Kelly, S. P. (2012a). Tight junctions, tight junction proteins and paracellular permeability across the gill epithelium of fishes: a review. *Respir. Physiol. Neurobiol.* **184**, 269–281.
- Chasiotis, H., Kolosov, D. and Kelly, S. P. (2012b). Permeability properties of the teleost gill epithelium under ion-poor conditions. *Am. J. Physiol. Regul. Integr. Comp. Physiol.* **302**, R727–R739.
- Cordenonsi, M., Mazzon, E., De Rigo, L., Baraldo, S., Meggio, F. and Citi, S. (1997). Occludin dephosphorylation in early development of *Xenopus laevis*. *J. Cell Sci.* **110**, 3131–3139.
- Cox, T. C. and Alvarado, R. H. (1979). Electrical and transport characteristics of skin of larval *Rana catesbeiana*. *Am. J. Physiol. Regul. Integr. Comp. Physiol.* **237**, R74–R79.
- Cummins, P. M. (2012). Occludin: one protein, many forms. *Mol. Cell. Biol.* **32**, 242–250.
- De Benedetto, A., Rafaels, N. M., McGirt, L. Y., Ivanov, A. I., Georas, S. N., Cheadle, C., Berger, A. E., Zhang, K., Vidyasagar, S., Yoshida, T. et al. (2011). Tight junction defects in patients with atopic dermatitis. *J. Allergy Clin. Immunol.* **127**, 773–86.e1–7.
- Ehrenfeld, J. and Klein, U. (1997). The key role of the H<sup>+</sup> V-ATPase in acid-base balance and Na<sup>+</sup> transport processes in frog skin. *J. Exp. Biol.* **200**, 247–256.
- Evans, M. J., Von Hahn, T., Tscherner, D. M., Syder, A. J., Panis, M., Wölk, B., Hatzioannou, T., McKeating, J. A., Bieniasz, P. D. and Rice, C. M. (2007). Claudin-1 is a hepatitis C virus co-receptor required for a late step in entry. *Nature* **446**, 801–805.
- Feldman, G. J., Mullin, J. M. and Ryan, M. P. (2005). Occludin: structure, function and regulation. *Adv. Drug Deliv. Rev.* **57**, 883–917.
- Fesenko, I., Kurth, T., Sheth, B., Fleming, T. P., Citi, S. and Hausen, P. (2000). Tight junction biogenesis in the early *Xenopus* embryo. *Mech. Dev.* **96**, 51–65.
- Fisher, M. C., Garner, T. W. J. and Walker, S. F. (2009). Global emergence of *Batrachochytrium dendrobatidis* and amphibian chytridiomycosis in space, time, and host. *Annu. Rev. Microbiol.* **63**, 291–310.
- Förster, C., Silwedel, C., Golenhofen, N., Burek, M., Kietz, S., Mankertz, J. and Drenckhahn, D. (2005). Occludin as direct target for glucocorticoid-induced improvement of blood-brain barrier properties in a murine in vitro system. *J. Physiol.* **565**, 475–486.
- Fujii, N., Matsuo, Y., Matsunaga, T., Endo, S., Sakai, H., Yamaguchi, M., Yamazaki, Y., Sugatani, J. and Ikari, A. (2016). Hypotonic stress-induced down-regulation of claudin-1 and -2 mediated by dephosphorylation and clathrin-dependent endocytosis in renal tubular epithelial cells. *J. Biol. Chem.* **291**, 24787–24799.
- Fujita, K., Katahira, J., Horiguchi, Y., Sonoda, N., Furuse, M. and Tsukita, S. (2000). *Clostridium perfringens* enterotoxin binds to the second extracellular loop of claudin-3, a tight junction integral membrane protein. *FEBS Lett.* **476**, 258–261.
- Fukumatsu, M., Ogawa, M., Arakawa, S., Suzuki, M., Nakayama, K., Shimizu, S., Kim, M., Mimuro, H. and Sasakawa, C. (2012). *Shigella* targets epithelial tricellular junctions and uses a noncanonical clathrin-dependent endocytic pathway to spread between cells. *Cell Host Microbe*, **11**, 325–336.
- Furuse, M., Hirase, T., Itoh, M., Nagafuchi, A., Yonemura, S., Tsukita, S. and Tsukita, S. (1993). Occludin: a novel integral membrane protein localizing at tight junctions. *J. Cell Biol.* **123**, 1777–1788.
- Furuse, M., Fujita, K., Hiragi, T., Fujimoto, K. and Tsukita, S. (1998). Claudin-1 and -2: novel integral membrane proteins localizing at tight junctions with no sequence similarity to occludin. *J. Cell Biol.* **141**, 1539–1550.
- Furuse, M., Hata, M., Furuse, K., Yoshida, Y., Haratake, A. and Sugitani, Y. (2002). Claudin-based tight junctions are crucial for the mammalian epidermal barrier: a lesson from claudin-1-deficient mice. *J. Cell Biol.* **156**, 1099–1111.
- Gauberg, J., Kolosov, D. and Kelly, S. P. (2017). Claudin tight junction proteins in rainbow trout (*Oncorhynchus mykiss*) skin: Spatial response to elevated cortisol levels. *Gen. Comp. Endocrinol.* **240**, 214–226.
- Gonzalez-Mariscal, L., Betanzos, A., Nava, P. and Jaramillo, B. E. (2003). Tight junction proteins. *Prog. Biophys. Mol. Biol.* **81**, 1–44.
- Greenspan, S. E., Longcore, J. E. and Calhoun, A. J. K. (2012). Host invasion by *Batrachochytrium dendrobatidis*: fungal and epidermal ultrastructure in model anurans. *Dis. Aquat. Org.* **100**, 201–210.
- Günzel, D. and Fromm, M. (2012). Claudins and other tight junction proteins. *Comp. Physiol.* **2**, 1819–1852.
- Günzel, D. and Yu, A. S. L. (2013). Claudins and the modulation of tight junction permeability. *Physiol. Rev.* **93**, 525–569.
- Guttman, J. A. and Finlay, B. B. (2009). Tight junctions as targets of infectious agents. *Biochim. Biophys. Acta* **1788**, 832–841.
- Hadj-Rabia, S., Baala, L., Vabres, P., Hamel-Teillac, D., Jacquemin, E., Fabre, M., Lyonnet, S., De Prost, Y., Munnich, A., Hadchouel, M. et al. (2004). Claudin-1 gene mutations in neonatal sclerosing cholangitis associated with ichthyosis: a tight junction disease. *Gastroenterology* **127**, 1386–1390.
- Hillyard, S. D., Møbjerg, N., Tanaka, S. and Larsen, E. H. (2008). Osmotic and ionic regulation in amphibians. In *Osmotic and Ionic Regulation: Cells and Animals* (ed. D. H. Evans), pp. 367–441. Florida, USA: CRC Press.
- Ikenouchi, J., Furuse, M., Furuse, K., Sasaki, H., Tsukita, S. and Tsukita, S. (2005). Tricellulin constitutes a novel barrier at tricellular contacts of epithelial cells. *J. Cell Biol.* **171**, 939–945.
- Katahira, J., Inoue, N., Horiguchi, Y., Matsuda, M. and Sugimoto, N. (1997). Molecular cloning and functional characterization of the receptor for *Clostridium perfringens* enterotoxin. *J. Cell Biol.* **136**, 1239–1247.
- Kelly, S. P. and Wood, C. M. (2001). Effect of cortisol on the physiology of cultured pavement cell epithelia from freshwater trout gills. *Am. J. Physiol. Regul. Integr. Comp. Physiol.* **281**, 811–820.

- Kielgast, F., Schmidt, H., Braubach, P., Winkelmann, V. E., Thompson, K. E., Frick, M., Dietl, P. and Wittekindt, O. H. (2016). Glucocorticoids regulate tight junction permeability of lung epithelia by modulating Claudin 8. *Am. J. Respir. Cell Mol. Biol.* **54**, 707-717.
- Kilpatrick, A. M., Briggs, C. J. and Daszak, P. (2010). The ecology and impact of chytridiomycosis: an emerging disease of amphibians. *Trends Ecol. Evol.* **25**, 109-118.
- Kirchmeier, P., Sayar, E., Hotz, A., Hausser, I., Islek, A., Yilmaz, A., Artan, R. and Fischer, J. (2014). Novel mutation in the CLDN1 gene in a Turkish family with Neonatal Ichthyosis Sclerosing Cholangitis (NISCH) syndrome. *Br. J. Dermatol.* **170**, 976-978.
- Kirschner, N., Poetzi, C., Den Driesch, P. V., Wladykowski, E., Moll, I., Behne, M. J. and Brandner, J. M. (2009). Alteration of tight junction proteins is an early event in psoriasis putative involvement of proinflammatory cytokines. *Am. J. Pathol.* **175**, 1095-1106.
- Klein, S. L., Strausberg, R. L., Wagner, L., Pontius, J., Clifton, S. W. and Richardson, P. (2002). Genetic and genomic tools for *Xenopus* research: the NIH *Xenopus* initiative. *Dev. Dyn.* **225**, 384-391.
- Kobayashi, K., Tsugami, Y., Matsunaga, K., Oyama, S., Kuki, C. and Kumura, H. (2016). Prolactin and glucocorticoid signaling induces lactation-specific tight junctions concurrent with  $\beta$ -casein expression in mammary epithelial cells. *Biochim. Biophys. Acta Mol. Cell Res.* **1863**, 2006-2016.
- Köhler, H., Sakaguchi, T., Hurley, B. P., Kase, B. J., Reinecker, H.-C. and McCormick, B. A. (2007). Salmonella enterica serovar Typhimurium regulates intercellular junction proteins and facilitates transepithelial neutrophil and bacterial passage. *AJP Gastrointest. Liver Physiol.* **293**, G178-G187.
- Kolosov, D. and Kelly, S. P. (2013). A role for tricellulin in the regulation of gill epithelium permeability. *Am. J. Physiol. Regul. Integr. Comp. Physiol.* **304**, R1139-R1148.
- Kolosov, D. and Kelly, S. P. (2017). Claudin-8d is a cortisol-responsive barrier protein in the gill epithelium of trout. *J. Mol. Endocrinol.* **59**, 1-12.
- Kolosov, D. and Kelly, S. P. (2018). Tricellular tight junction-associated angulins in the gill epithelium of rainbow trout. *Am. J. Physiol. Regul. Integr. Comp. Physiol.* **315**, R312-R322.
- Kolosov, D., Bui, P., Donini, A., Wilkie, M. P. and Kelly, S. P. (2017a). A role for tight junction-associated MARVEL proteins in larval sea lamprey (*Petromyzon marinus*) osmoregulation. *J. Exp. Biol.* **220**, 3657-3670.
- Kolosov, D., Donini, A. and Kelly, S. P. (2017b). Claudin-31 contributes to corticosteroid-induced alterations in the barrier properties of the gill epithelium. *Mol. Cell. Endocrinol.* **439**, 457-466.
- Krug, S. M., Amasheh, S., Richter, J. F., Milatz, S., Günzel, D., Westphal, J. K., Huber, O., Shulzke, J. D. and Fromm, M. (2009). Tricellulin forms a barrier to macromolecules in tricellular tight junctions without affecting ion permeability. *Mol. Biol. Cell* **20**, 3713-3724.
- Krug, S. M., Bojarski, C., Fromm, A., Lee, I. M., Dames, P., Richter, J. F., Turner, J. R. and Fromm, M. (2018). Tricellulin is regulated via interleukin-13-receptor  $\alpha 2$ , affects macromolecule uptake, and is decreased in ulcerative colitis. *Mucosal Immunol.* **11**, 345-356.
- Liu, Y., Beyer, A. and Aebersold, R. (2016). On the dependency of cellular protein levels on mRNA abundance. *Cell* **165**, 535-550.
- Mandel, L. J. and Curran, P. F. (1972). Chloride flux via a shunt pathway in frog skin: apparent exchange diffusion. *Biochim. Biophys. Acta* **282**, 258-264.
- Mariano, C., Sasaki, H., Brites, D. and Brito, M. A. (2011). A look at Tricellulin and its role in tight junction formation and maintenance. *Eur. J. Cell Biol.* **90**, 787-796.
- Martinez-Palomo, A., Elij, D. and Bracho, H. (1971). Localization of permeability barriers in the frog skin epithelium. *J. Cell Biol.* **50**, 277-287.
- Masuda, R., Semba, S., Mizuuchi, E., Yanagihara, K. and Yokozaki, H. (2010). Negative regulation of the tight junction protein tricellulin by snail-induced epithelial-mesenchymal transition in gastric carcinoma cells. *Pathobiology* **77**, 106-113.
- McLaughlin, J., Padfield, P. J., Burt, J. P. H. and O'Neill, C. A. (2004). Ochratoxin A increases permeability through tight junctions by removal of specific claudin isoforms. *Am. J. Physiol. Cell Physiol.* **287**, C1412-C1417.
- McLaughlin, J., Lambert, D., Padfield, P. J., Burt, J. P. H. and O'Neill, C. A. (2009). The mycotoxin patulin, modulates tight junctions in caco-2 cells. *Toxicol. Vitr.* **23**, 83-89.
- Muza-Moons, M. M., Schneeberger, E. E. and Hecht, G. A. (2004). Enteropathogenic *Escherichia coli* infection leads to appearance of aberrant tight junction strands in the lateral membrane of intestinal epithelial cells. *Cell. Microbiol.* **6**, 783-793.
- Parsons, R. H. and Mobin, F. (1991). Water flow across the pectoral and ventral pelvic patch in *Rana catesbeiana*. *Physiol. Zool.* **64**, 812-822.
- Pessier, A. P., Nichols, D. K., Longcore, J. E. and Fuller, M. S. (1999). Cutaneous chytridiomycosis in poison dart frogs (*Dendrobates* spp.) and White's tree frogs (*Litoria caerulea*). *J. Vet. Diagn. Invest.* **11**, 194-199.
- Peterson, J. D., Steffen, J. E., Reinert, L. K., Cobine, P. A., Appel, A., Rollins-Smith, L. and Mendonça, M. T. (2013). Host stress response is important for the pathogenesis of the deadly amphibian disease, chytridiomycosis, in *Litoria caerulea*. *PLoS ONE* **8**, 1-7.
- Raleigh, D. R., Marchiando, A. M., Zhang, Y., Shen, L., Sasaki, H., Wang, Y., Long, M. and Turner, J. R. (2010). Tight junction-associated MARVEL proteins marvelD3, tricellulin, and occludin have distinct but overlapping functions. *Mol. Biol. Cell* **21**, 1200-1213.
- Robertson, S. L., Smedley, J. G. and McClane, B. A. (2010). Identification of a Claudin-4 residue important for mediating the host cell binding and action of *Clostridium perfringens* enterotoxin. *Infect. Immun.* **78**, 505-517.
- Rollins-Smith, L. A. (2017). Amphibian immunity—stress, disease, and climate change. *Dev. Comp. Immunol.* **66**, 111-119.
- Rosenblum, E. B., Stajich, J. E., Maddox, N. and Eisen, M. B. (2008). Global gene expression profiles for life stages of the deadly amphibian pathogen *Batrachochytrium dendrobatidis*. *Proc. Natl. Acad. Sci. USA* **105**, 17034-17039.
- Saharinen, P., Helotera, H., Miettinen, J., Norrmén, C., D'Amico, G., Jeltsch, M., Langenberg, T., Vandevelde, W., Ny, A., Dewerchin, M. et al. (2010). Claudin-like protein 24 interacts with the VEGFR-2 and VEGFR-3 pathways and regulates lymphatic vessel development. *Genes Dev.* **24**, 875-880.
- Singer, K. L., Stevenson, B. R., Woo, P. L. and Firestone, G. L. (1994). Relationship of serine/threonine phosphorylation/dephosphorylation signaling to glucocorticoid regulation of tight junction permeability and ZO-1 distribution in nontransformed mammary epithelial cells. *J. Biol. Chem.* **269**, 16108-16115.
- Sourisseau, M., Michta, M. L., Zony, C., Israelow, B., Hopcraft, S. E., Narbus, C. M., Parra Martin, A. and Evans, M. J. (2013). Temporal analysis of hepatitis C virus cell entry with occludin directed blocking antibodies. *PLoS Pathog.* **9**, e1003244.
- Stuart, S. N., Chanson, J. S., Cox, N. A., Young, B. E., Rodrigues, A. S. L., Fischman, D. L. and Waller, R. W. (2004). Status and trends of amphibian declines and extinctions worldwide. *Science* **306**, 1783-1786.
- Sun, J., Wang, X., Li, C. and Mao, B. (2015). *Xenopus* Claudin-6 is required for embryonic pronephros morphogenesis and terminal differentiation. *Biochem. Biophys. Res. Commun.* **462**, 178-183.
- Symonds, E. P., Trott, D. J., Bird, P. S. and Mills, P. (2008). Growth characteristics and enzyme activity in *Batrachochytrium dendrobatidis* isolates. *Mycopathologia* **166**, 143-147.
- Takahashi, S., Iwamoto, N., Sasaki, H., Ohashi, M., Oda, Y., Tsukita, S. and Furuse, M. (2009). The E3 ubiquitin ligase LNX1p80 promotes the removal of claudins from tight junctions in MDCK cells. *J. Cell Sci.* **122**, 985-994.
- Tokuda, S., Miyazaki, H., Nakajima, K., Yamada, T. and Marunaka, Y. (2010). NaCl flux between apical and basolateral side recruits claudin-1 to tight junction strands and regulates paracellular transport. *Biochem. Biophys. Res. Commun.* **393**, 390-396.
- Tokumasu, R., Tamura, A. and Tsukita, S. (2017). Time- and dose-dependent claudin contribution to biological functions: Lessons from claudin-1 in skin. *Tissue Barriers* **5**, 1-6.
- Van Rooij, P., Martel, A., Haesebrouck, F. and Pasmans, F. (2015). Amphibian chytridiomycosis: a review with focus on fungus-host interactions. *Vet. Res.* **46**, 1-22.
- Volksdorf, T., Heilmann, J., Eming, S. A., Schawjinski, K., Zorn-Kruppa, M., Ueck, C., Vidal-y-Sy, S., Windhorst, S., Jücker, M., Moll, I. et al. (2017). Tight junction proteins claudin-1 and occludin are important for cutaneous wound healing. *Am. J. Pathol.* **187**, 1301-1312.
- Voyles, J., Berger, L., Young, S., Speare, R., Webb, R., Warner, J., Rudd, D., Campbell, R. and Skerratt, L. F. (2007). Electrolyte depletion and osmotic imbalance in amphibians with chytridiomycosis. *Dis. Aquat. Organ.* **77**, 113-118.
- Voyles, J., Young, S., Berger, L., Campbell, C., Voyles, W. F., Dinudom, A., Cook, D., Webb, R., Alford, R. A., Skerratt, L. F. et al. (2009). Pathogenesis of chytridiomycosis, a cause of catastrophic amphibian declines. *Science* **326**, 582-585.
- Watanabe, H., Narai, A. and Shimizu, M. (1999). Purification and cDNA cloning of a protein derived from *Flammulina velutipes* that increases the permeability of the intestinal Caco-2 cell monolayer. *Eur. J. Biochem.* **262**, 850-857.
- Welinder, C. and Ekblad, L. (2010). Coomassie staining as loading control in western blot analysis Coomassie staining as loading control in western blot analysis. *J. Proteome Res.* **10**, 1416-1419.
- Wu, N. C., Cramp, R. L. and Franklin, C. E. (2018). Body size influences energetic and osmoregulatory costs in frogs infected with *Batrachochytrium dendrobatidis*. *Sci. Rep.* **8**, 1-11.
- Yamagishi, M., Ito, Y., Ariizumi, T., Komazaki, S., Danno, H., Michiue, T. and Asashima, M. (2010). Claudin5 genes encoding tight junction proteins are required for *Xenopus* heart formation. *Dev. Growth Differ.* **52**, 665-675.
- Yu, A. S. L., McCarthy, K. M., Francis, S. A., McCormack, J. M., Lai, J., Rogers, R. A., Lynch, R. D. and Schneeberger, E. E. (2005). Knockdown of occludin expression leads to diverse phenotypic alterations in epithelial cells. *Am. J. Physiol. Cell Physiol.* **288**, C1231-C1241.
- Yuki, T., Haratake, A., Koishikawa, H., Morita, K., Miyachi, Y. and Inoue, S. (2007). Tight junction proteins in keratinocytes: Localization and contribution to barrier function. *Exp. Dermatol.* **16**, 324-330.